https://doi.org/10.5194/egusphere-2025-5934
Preprint. Discussion started: 11 February 2026

Channel Dynamics in an Experimental Alluvial Fan Under Constant Boundary Conditions: A Classification of Avulsion and Lateral Migration Events

Nastaran Nematollahi[1, 2], Brett Eaton[1, 2], and Sarah Davidson[1, 2]

[1]Department of Geography, University of British Columbia, 1984 West Mall, Vancouver, BC V6T 1Z2, Canada
[2]BGC Engineering Inc., 980 Howe Street, Vancouver, BC V6Z 0C8, Canada

Correspondence: Nastaran Nematollahi (nasipour@student.ubc.ca)

Abstract. Alluvial fans exhibit complex channel dynamics, spanning gradual lateral migration to sudden avulsions. Although allogenic processes are recognized as key drivers of these behaviors, the autogenic mechanisms regulating channel change remain poorly understood. In this study, we present a quantitative analysis of the main channel kinematics on a widely graded, non-cohesive experimental alluvial fan, utilizing high-temporal-resolution RGB imagery and main channel centerline tracking. By employing two key metrics—displacement magnitude (normalized by channel width) and flow continuity, defined as the degree of overlap in the active channel footprint from one image to the next—we move beyond qualitative assessments, which are often subject to researcher bias, and establish a clear framework for distinguishing between migratory (continuous) and avulsive (discrete) channel behaviours. Our findings reveal that the fan alternates between supply-limited phases, when a small number of efficient channels route sediment to the toe with only localized reworking, and transport-limited phases, when a more complex, inefficient channel network traps sediment mid-fan, favoring abrupt reorganizations (i.e., avulsions). Contrary to the conventional assumption that systematic aggradation from toe to apex triggers large-scale channel abandonment, we demonstrate that lateral sediment redistribution often prevents fan-wide sediment buildup, thereby delaying or even preventing major avulsions. These results highlight the critical role of self-regulating autogenic processes, particularly the lateral reworking of coarse sediment, in controlling both the timing and scale of channel adjustments, emphasizing the need to incorporate localized feedback mechanisms into predictive models to improve our understanding of alluvial fan dynamics.

1 Introduction

Depositional environments such as alluvial fans and fan deltas often exhibit a quasi-radial pattern of deposition created by the spreading of incoming sediment in response to reduced confinement, slope transitions, and changing boundary conditions (Harvey, 2010; Bull, 1979; Mackey and Bridge, 1995). Superimposed on this fan-scale geometry, a dynamic network of active channels migrates laterally and occasionally undergoes abrupt relocation, shaping overall fan morphology (Jerolmack and Mohrig, 2007; Jobe et al., 2016; Slingerland and Smith, 2004).

Across many depositional systems, short-lived channel adjustments—such as bar migration, bank erosion, or shifts in individual flow threads—are confined to a narrow corridor of activity only a few channel widths wide, commonly referred to as the channel belt. These localized adjustments operate continuously and incrementally, redistributing sediment without necessarily reorganizing the fan surface (Ashmore, 2013). Over longer timescales, however, the repeated lateral motion can accumulate so that reworking spreads beyond the channel belt, and affects a large portion of the fan surface (Cazanacli et al., 2022). By contrast, avulsions represent discrete, abrupt changes in which a channel abandons its established corridor and relocates to a new course (Mohrig et al., 2000; Ashmore, 1991). Avulsions may be spatially limited, as in localized avulsions where flow is diverted into an adjacent chute or braid thread, or fan-scale, as in major avulsions that initiate the growth of a new lobe. Bifurcation, the division of flow into two or more downstream branches, often acts as a decision point between different modes of channel adjustment. When bifurcations are stable, multiple threads can coexist and migrate incrementally, whereas unstable bifurcations typically result in one branch capturing flow, leading to channel abandonment and avulsion (Burge, 2006).

Conventional studies suggest that avulsion is typically driven by two key processes: (1) superelevation, where in-channel sediment aggradation exceeds that of the surrounding floodplain, progressively raising the channel relative to adjacent floodplain, and (2) backfilling, in which upstream-migrating waves of sediment reduce channel capacity, promoting overflow into a new pathway (Mohrig et al., 2000; Bryant et al., 1995; Clarke et al., 2010; Reitz et al., 2010). Both mechanisms imply that avulsion frequency is often tied to the time required to fill a channel with sediment. For a given channel depth, the avulsion timescale is proportional to the channel depth and inversely related to the aggradation rate (Jerolmack and Mohrig, 2007). Recent work also demonstrates that channel relocation need not be abrupt. Instead, channels can shift progressively through a sequence of lateral adjustments, a process termed sweeping (Sylvester et al., 2019; Cazanacli et al., 2022). Under this interpretation, repeated small lateral shifts can integrate over time into a net relocation, so channel abandonment can emerge from sustained migration rather than a single threshold-style jump

From a stratigraphic perspective, changes in channel position—whether gradual or abrupt—are critical for redistributing water and sediment across floodplains, ultimately shaping fluvial architectures. However, from a geohazard standpoint, distinguishing between these processes is essential because each responds differently to environmental factors such as sea-level rise and variations in sediment supply (Jerolmack and Mohrig, 2007; Slingerland and Smith, 2004; Harvey, 2010). For instance, sea-level rise can promote delta-top aggradation and increase channel avulsion rates, as demonstrated by laboratory experiments (Jerolmack, 2009; Martin et al., 2009). In contrast, studies of non-avulsive settings show that channel migration rates may remain stable or even decline during sea-level rise (Bufe et al., 2019; Wickert et al., 2013). Instead, these areas often exhibit migration patterns that are more sensitive to changes in downstream sediment flux (Constantine et al., 2014; Wickert et al., 2013).

Both internal (autogenic) and external (allogenic) factors shape channel evolution on alluvial fans (Schumm et al., 1987; Clarke et al., 2010; Reitz and Jerolmack, 2012). Autogenic processes include local changes in slope, sediment deposition, and channel geometry that self-organize within the fan, whereas allogenic forces—such as climatic shifts, tectonics, and human interventions—induce broader environmental changes that alter flow conditions. Much of our understanding about fan dynamics, particularly autogenic behavior, comes from experiments and field studies, but many interpretations have historically been qualitative. Early laboratory and field studies (e.g., (Schumm et al., 1987; Whipple et al., 1998; Hooke, 1968)) relied on visual observations and sparse measurement grids, providing pioneering but coarse-resolution insights into fan-building processes. In

https://doi.org/10.5194/egusphere-2025-5934
Preprint. Discussion started: 11 February 2026

recent years, high-resolution topographic surveys (Miller et al., 2019; Reitz and Jerolmack, 2012) have provided finer spatial detail; however, their relatively coarse temporal sampling (on the order of 15 minutes) still misses many short-lived changes. More recently, using high-frequency, high-resolution topographic data, Leenman and Eaton (2021) captured the complex nature of fan behavior beyond period cycles; however, distinguishing gradual channel migration from abrupt channel relocation remains challenging due to their pixel-based wet/dry event classification.

Another limitation in many fan experiments is the simplification of the sediment. Many experimental studies of alluvial fans have used narrowly graded sediment mixtures (sand-only or bimodal setups), thereby reducing the wide grain-size variability observed in natural fans (e.g., (Schumm et al., 1987; Reitz and Jerolmack, 2012; Reitz et al., 2010). Such mixtures can reproduce fan building at a basic level; however, they often underrepresent mechanical interlocking that occurs with a broad range of grain sizes, resulting in channels with easily erodible margins that tend to form unconfined sheet flow. Consistent with this, Booker and Eaton (2020) demonstrated that narrowly graded mixtures cannot reproduce the morphodynamics observed in a widely graded mixture with the same median grain size D_{50}.

This study investigates the dynamics of a widely graded experimental alluvial fan constructed under constant discharge and sediment supply, focusing on the displacement of the main channel over time and space. While smaller side channels might fill more quickly and be more prone to shift, the changes they induce are relatively localized and less significant in reshaping the fan's large-scale structure compared to the main channel. This is analogous to the concept of "formative flow" described by Davidson and Eaton (2018), in which larger, less frequent flows shape channel form, whereas "effective flows" transport most sediment over time but have a lesser impact on morphology (Wolman, 1960). By tracking channel displacement at high temporal resolution (every minute), we establish a conceptual framework for distinguishing gradual, bank-erosion-driven channel migrations (continuous in both time and space) from abrupt, avulsive relocations (discrete shifts in channel position). Our primary question is how often the channel migrates gradually versus avulsing abruptly under these steady-input but highly dynamic conditions. We hypothesize that continuous sediment redistribution within a confined corridor inhibits the bed aggradation needed for sudden, discrete channel reoccupation elsewhere on the fan.

To test this, we map the main flow path in each image at one-minute intervals and quantify both the magnitude and direction of channel displacement. We then compare the cumulative net shifts associated with gradual migration to the single, larger displacements that define avulsions, thereby clarifying whether the channel shifts abruptly due to localized deposition or more diffuse erosion. This approach provides a more explicit link between how the main channel reworks the fan surface and why such reworking occurs under steady conditions, offering new insights into the autogenic processes that control fan evolution. By clarifying the interplay between gradual and abrupt channel shifts, these findings facilitate more accurate stratigraphic interpretations of fan deposits and enhance hazard assessments in settings prone to rapid channel reconfiguration.

https://doi.org/10.5194/egusphere-2025-5934
Preprint. Discussion started: 11 February 2026

2 Methods

2.1 Experimental Set-up

We conducted the experiment using a physical model representing a typical gravel-cobble alluvial fan at the University of British Columbia. We used a fan table with dimensions of 2.4 meters by 2.4 meters and a height of 0.2 meters. The table was equipped with a feeder channel, which measured 0.2 meters by 0.5 meters by 0.18 meters, centrally located along one wall of the table and a conveyor belt sediment feeder next to it (as shown in Fig. 1). Water was supplied from a constant-head tank with adjustable outflow. Sediment and water were mixed in a funnel and delivered to the feeder-channel inlet. We allowed sediment to aggrade and degrade freely in the feeder channel, as in a natural system. The discharge and sediment supply were held constant at 100 mL/s and 2 g/s, respectively, throughout the experiment, resulting in a sediment concentration of 1.1% by volume, characteristic of clear-water floods rather than debris-flow conditions (Church and Jakob, 2020). We set the fan table gradient at 0.01 (m/m) to ensure efficient drainage away from the fan's edge. The sediment mixture was widely graded (0.25–8 mm), with a median size D_{50} of 0.6 mm and D_{95} of 2.3 mm (Fig. 2). The experiment ran for a total of 9 hours. The first 3.5 hours served as a baseline setup period, after which we began detailed observation and analysis of fan development and channel dynamics.

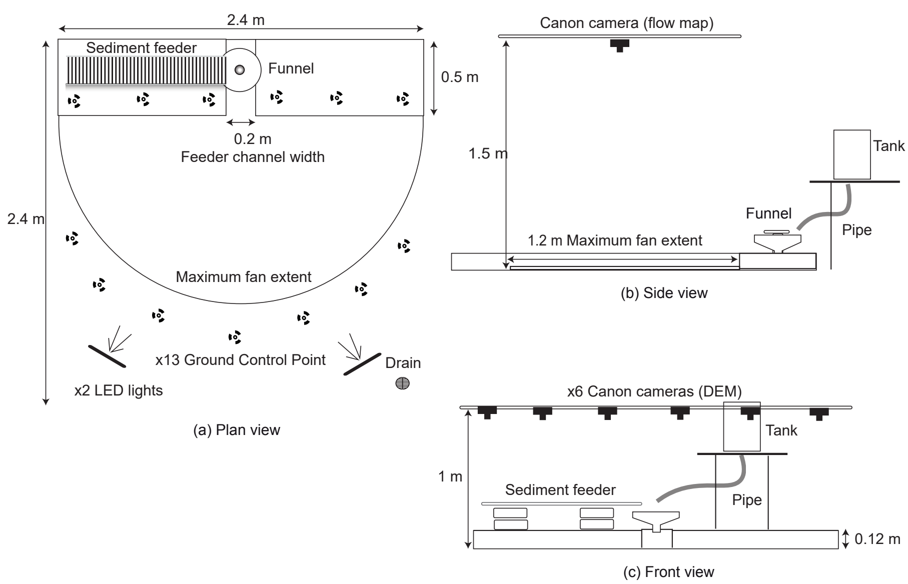

Figure 1. Experimental setup: (a) plan view, (b) side view, and (c) front view.

https://doi.org/10.5194/egusphere-2025-5934
Preprint. Discussion started: 11 February 2026

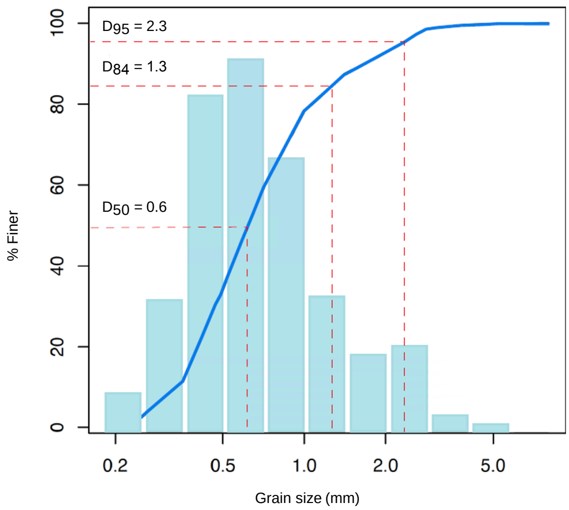

Figure 2. Grain size distribution (GSD) of the sand and fine gravel mixture in the experiments.

2.2 Analysis

We briefly summarize our data-processing workflow here. Optical flow analyses were performed in Python using OpenCV (Bradski, 2000), while all other analyses were conducted in R (R Core Team, 2025). All scripts, along with a representative subset of the experimental dataset, are available in our GitHub repository: https://github.com/Nastarannmt?tab=repositories.

2.2.1 Data Collection and Optical Flow Analysis

We used a centrally mounted overhead camera system positioned above the fan table to document the structure of the flow with high temporal resolution, capturing images every three seconds throughout the experiment. These images were compiled into one-minute time-lapse videos, each containing 20 frames. To identify active flow zones, we applied Farnebäck dense optical flow (FDOF) (Farneback, 2000), which estimates pixel-wise motion between consecutive frames based on two assumptions: (1) gray-level constancy, where pixel intensities remain stable over short intervals, and (2) velocity smoothness, where neighboring pixels exhibit similar motion. FDOF minimizes the intensity difference between successive frames, as expressed by the following equation:

$$E = \iint \left[I_2(x + \boldsymbol{d}) - I_1(x)\right]^2, dx, \tag{1}$$

where $I_1(x)$ and $I_2(x)$ are the intensity values at position x in the first and second frames, respectively, and d is the displacement vector (Farneback, 2000). We implemented the algorithm in Python using OpenCV's `cv2.calcOpticalFlowFarneback`

https://doi.org/10.5194/egusphere-2025-5934
Preprint. Discussion started: 11 February 2026

Table 1. Optical flow input parameters used in this study.

Parameter	Value
Pyramidal scaling	0.5
Number of pyramid levels	3
Window size	15×15 pixels
Iterations	3
Polynomial expansion size	5
Smoothing factor	1.2

function. Before calculating flow, each frame was converted to grayscale and smoothed with a 5×5 Gaussian kernel to reduce noise. The parameters used are summarized in Table 1.

The algorithm produces a dense field of motion vectors, where each pixel is assigned a vector $\boldsymbol{v} = (u, v)$, representing its estimated displacement between two consecutive frames. From this vector, both the magnitude and direction of motion are derived as:

$$|\boldsymbol{v}| = \sqrt{u^2 + v^2}, \tag{2}$$

$$\theta = \arctan\left(\frac{v}{u}\right). \tag{3}$$

For each one-minute sequence (20 frames), we computed 19 frame-to-frame flow fields and averaged per-pixel magnitudes to obtain a mean-motion raster, $\overline{|\mathbf{u}|}$. Dense optical flow is highly sensitive to sub-pixel intensity changes, which means it can also detect low-amplitude noise in areas where flow is slow or ponded, but it produces stronger motion signals and thus higher contrast in regions of actively flowing water. Initial tests showed that applying a 75th-percentile threshold to $\overline{|\mathbf{u}|}$ preserved active cells while filtering out quasi-static water patches that color-thresholding missclassifies as active (Leenman and Eaton, 2021). Based on these tests, we implemented a two-step thresholding in which we first retained only those pixels where $\overline{|\mathbf{u}|} \geq Q_{0.75}$, and then performed clump-based segmentation to remove small, isolated pixel clusters (Fig. 3).

Although our primary analyses relied on overhead imagery and optical flow techniques, we also generated digital elevation models (DEMs) to validate and contextualize our observations. DEMs were created using an adaptation of Structure-from-Motion (SfM) photogrammetry (Fonstad et al., 2013; Westoby et al., 2012). Six Canon EOS Rebel T6i DSLRs with EF-S 18–55 mm lenses were mounted on a rail system above the table, taking photos every 10 cm with at least 85% stereo overlap. Photographs were acquired at 30-minute intervals after stopping the water flow and allowing the fan surface to drain. Thirteen ground control points ensured accurate georeferencing of the DEMs, achieving a resolution of 0.5 mm (details about the photogrammetry methods are provided in the supplementary material).

https://doi.org/10.5194/egusphere-2025-5934
Preprint. Discussion started: 11 February 2026

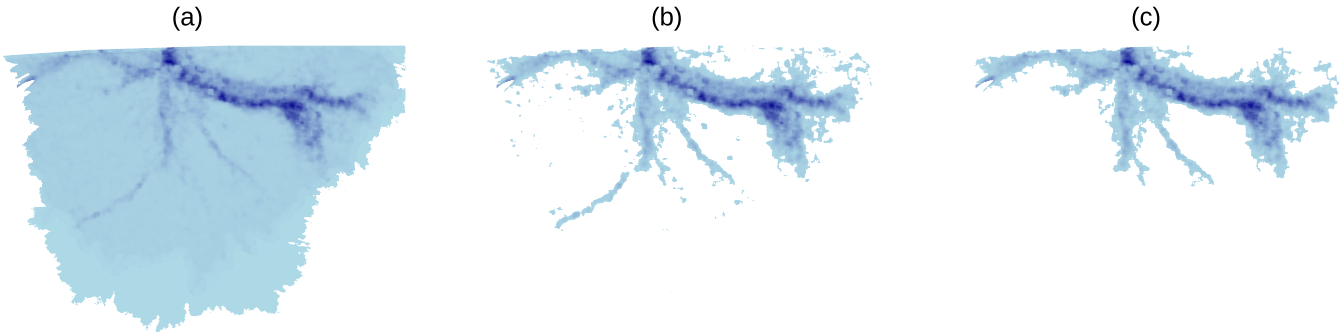

Figure 3. Visualization of active flow areas on the alluvial fan using Farnebäck optical flow analysis. (a) Raw optical flow motion values representing per-pixel displacement over one-minute intervals. (b) Thresholding at the 0.75 quantile to isolate significant flow activity. (c) Final flow map after removing noise through clump-based segmentation

2.2.2 Channel network detection

To define the centerlines of geomorphically active channels on the fan, we generated semicircular contour lines spaced at 2 cm intervals from the fan apex to the toe and extracted flow raster values along each contour line. We then applied the Density-Based Spatial Clustering of Applications with Noise (DBSCAN) algorithm in two stages. In the first stage, DBSCAN was applied along each semicircular contour to group points within a 2 cm neighborhood into clusters, representing individual channel transects (fig. 4. (b)). For each transect, we considered the motion magnitude of pixels within the channel and calculated the centroid of each cluster to approximate the thalweg location (fig. 4 (c)). In the second stage, DBSCAN was applied to these centroids along the radial direction of the fan. By clustering centroids within a 2 cm radius, we connected individual channel transects into continuous paths, representing channel segments.

Further, the channel segments were connected based on their proximity, with the starting point of each channel segment linked to its nearest upstream neighboring channel segment. Channels were then labelled according to their Total Motion Contribution (TMC), calculated as the product of the average pixel motion and the total length of a channel, a proxy for the size of the channel (i.e. the volume of sediment transported and/or the volume of water carried in it). The channel with the highest TMC was designated as the main channel, with channel order increasing as average motion decreased, as shown in Figure 4 (f).

2.2.3 Main Channel Displacement Magnitude and Direction

To analyze the main channel displacement over time, the angular position of a point at two time steps (t_1 and t_2) is calculated as $\theta_1 = \arctan 2(Y_{t1}, X_{t1})$ and $\theta_2 = \arctan 2(Y_{t2}, X_{t2})$. The angular displacement, $\Delta\theta$, is then computed as the absolute difference between these angular positions: $\Delta\theta = |\theta_2 - \theta_1|$. Since angular measurements are bounded within the range $-\pi$ to π, any displacement exceeding π is adjusted to fall within $[0, \pi]$ using the rule: $\Delta\theta = 2\pi - \Delta\theta$ if $\Delta\theta > \pi$, otherwise $\Delta\theta$ remains unchanged.

https://doi.org/10.5194/egusphere-2025-5934
Preprint. Discussion started: 11 February 2026

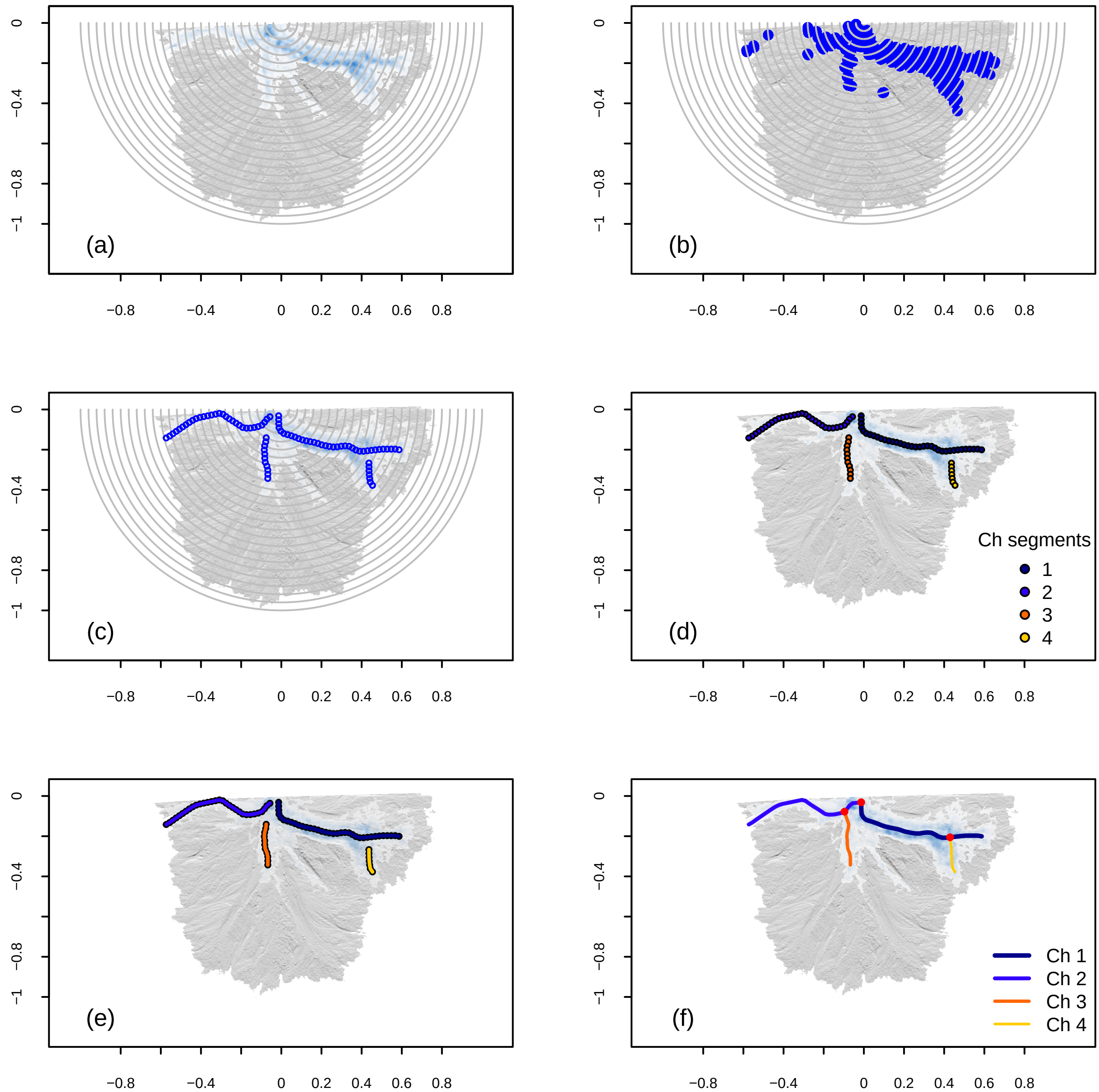

Figure 4. Channel detection and clustering on an experimental alluvial fan. (a) Initial flow data with semicircular contour lines (gray). (b) Result of adaptive thresholding, showing high-motion pixels above the average in each radial section. (c) Channel transects identified using DBSCAN clustering, with centroids marking the midpoints of each transect. (d) Final clustering of centroids to form continuous channel paths, with color-coded clusters representing distinct channels from the apex to the distal edge.

https://doi.org/10.5194/egusphere-2025-5934
Preprint. Discussion started: 11 February 2026

The direction of movement is determined using the signed value of $\Delta\theta$, where positive values indicate counterclockwise movement, and negative values indicate clockwise movement. The magnitude of displacement, expressed in units of channel length, is then calculated as the arc length $\text{Arc\_Length} = r \cdot \Delta\theta$, where r represents the radial distance of the point from the apex. The buffer width was determined by dividing the average flow width/the number of full length channels. The width of the main channel was calculated by dividing the area of active flow cells within the buffer by the length of the main channel.

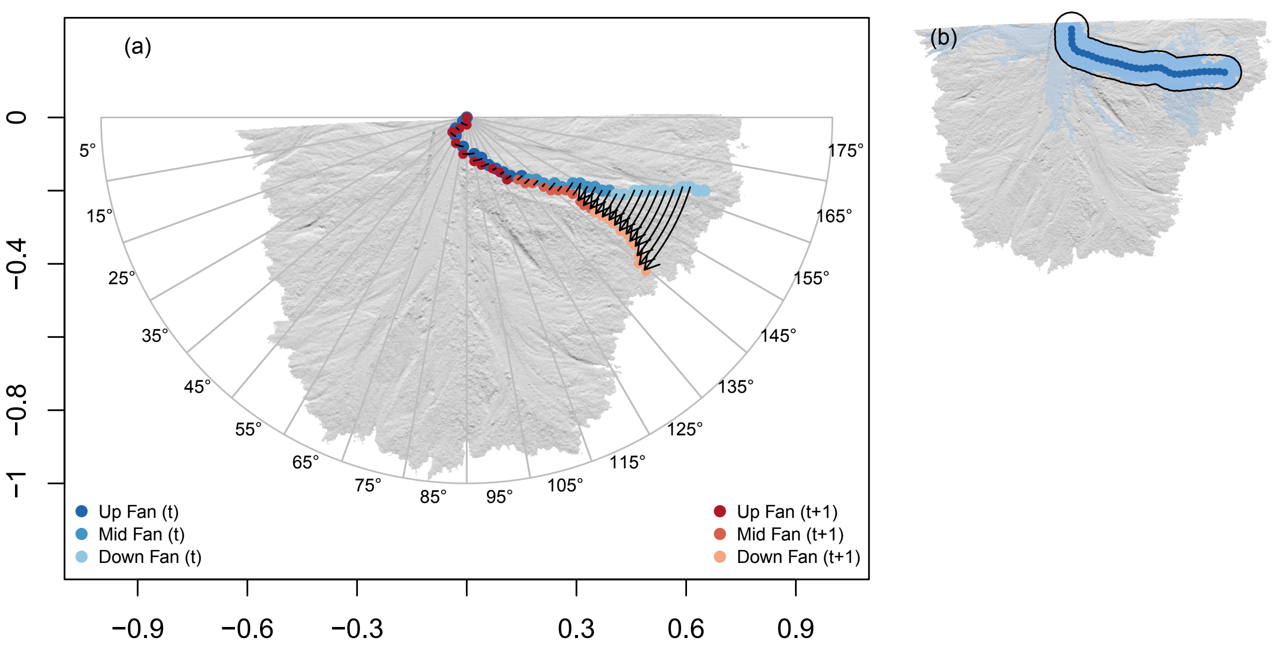

Figure 5. (a) Angular displacement of the main channel between minutes 216 and 217, overlaid on a hillshaded DEM acquired at the subsequent 30-minute scan.(b) Channel width estimates derived from buffered flow zones for the same time interval, overlaid on the same hillshaded DEM.

3 Result

3.1 Qualitative Observation

Throughout the 5.5 hours of the experiment, the flow zone appeared to migrate continuously, with variability in both timing and spatial extent. Based on visual inspection of time-lapse videos (see Supplementary Video) corresponding to the 5.5-hour experiment, we noted three qualitative patterns: (1) The main channel moved back and forth across different parts of the fan, occasionally sweeping over long distances before reversing direction. During these shifts, the channel oscillated in small steps

https://doi.org/10.5194/egusphere-2025-5934
Preprint. Discussion started: 11 February 2026

while showing a net drift in one direction, either clockwise or counterclockwise. (2) Certain portions of the channel, particularly in the lower fan region, exhibited more pronounced lateral movement than others. (3) The upper segment near the apex, by contrast, remained comparatively stable, although minor realignments still occurred intermittently.

3.2 Main channel displacement

To characterize the spatial and temporal behavior of the main channel, we quantified the active flow route's displacement in time and space. Specifically, we define $\Delta\theta$ as the instantaneous angular change of the channel centerline between consecutive images (recorded at one-minute intervals), with units of degrees per minute. $\Delta\theta$ is a proxy for the migration rate that accounts for fan geometry by expressing displacement as an angular change about the apex. Where necessary, we convert the angular shift into an equivalent displacement expressed in mean channel widths.

Figure 6 (a) displays $\Delta\theta$ for the up fan, mid fan, and down-fan sectors. The difference in angular shift distribution among the three locations indicates that the channel has a fairly complex mobility, with different sections moving at different rates. Furthermore, different parts of the channel (e.g., up-fan vs. down-fan) do not always move in the same direction. Additionally, the magnitude and variability of these shifts increase with distance from the apex. Near the apex, $\Delta\theta$ has smaller mean values (approximately $2^\circ\,\mathrm{min}^{-1}$) with a standard deviation of $\pm 4^\circ$, indicating frequent but minor channel displacements. In contrast, the mid-fan and down-fan regions exhibit larger and more variable shifts (standard deviations up to $\pm 7^\circ$), signifying greater channel instability and larger reworking events farther from the apex.

Within this mobile fan system, the $\Delta\theta$ time series alternates between two distinct patterns: low-mobility intervals (stable to slight displacement) and high-mobility intervals. The Low Mobility intervals, highlighted in gray in Figure 6 (a), occur when the main channel's average angular displacement falls below approximately $1.32^\circ, \mathrm{min}^{-1}$. These intervals often last for several minutes (sometimes up to 24 minutes, on average around 5 minutes), during which the channel occupies a relatively narrow corridor with negligible lateral movement. This behavior typically indicates near-equilibrium conditions, where the channel is effectively incised, transporting sediment efficiently, and any coarse or bar deposits remain small enough to be reworked quickly. Outside these low mobility intervals, the channel moves more rapidly at rates above $1.32^\circ, \mathrm{min}^{-1}$, often reversing direction and/or shifting over larger distances.

Figure 6 (b) shows the cumulative signed angular displacement $\Sigma\Delta\theta$, where positive slopes indicate counterclockwise shifts, and negative slopes represent clockwise movement. Near-horizontal segments correspond to low-mobility intervals during which the channel's net position remains largely confined and stable. By contrast, more moderate slopes suggest steady directional migration, and steep slopes reflect rapid realignments, which may reflect either continuous lateral migration, where the channel sweeps several sectors during the one-minute interval, reworking all sediment along its path, or abrupt avulsion, where the channel jumps to a new route, bypassing the previous corridor. Distinguishing between these mechanisms (continuous vs. discrete) requires additional analysis beyond the cumulative signal alone.

https://doi.org/10.5194/egusphere-2025-5934
Preprint. Discussion started: 11 February 2026

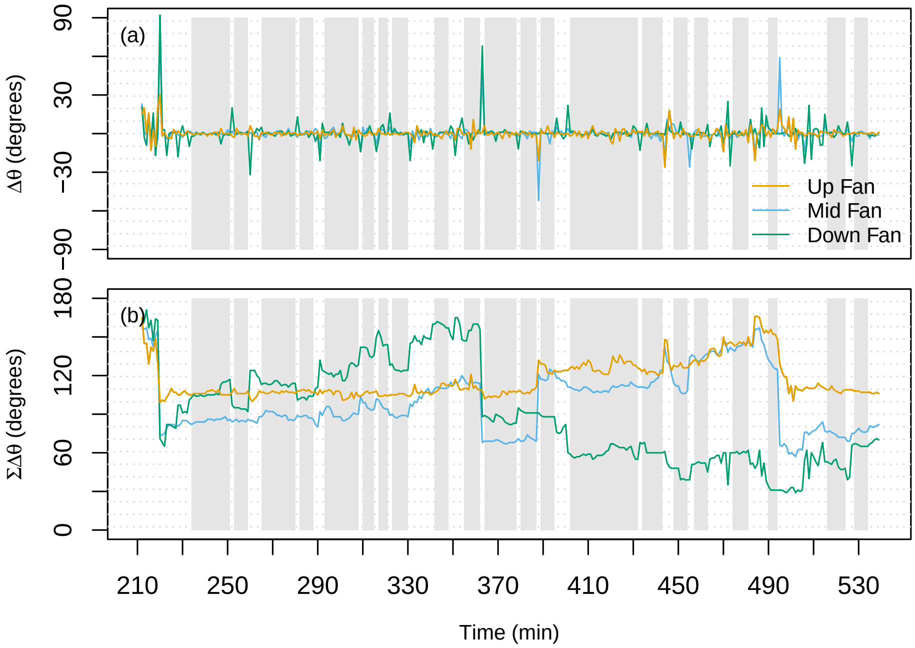

Figure 6. Time-resolved angular displacement of the main channel: (a) instantaneous angular displacement for the up-fan, mid-fan, and down-fan sectors, with gray-shaded periods denoting low-mobility intervals, (b) cumulative signed angular displacement, where positive slopes indicate counterclockwise shifts and negative slopes represent clockwise shifts.

3.3 Avulsion Classification Scheme

Building on the spatial and temporal patterns quantified above, we introduce a classification framework that separates the observed channel shifts into distinct behavioral types. We evaluate each channel shift according to:

(1) the arc length of channel displacement, normalized by a time-varying, experiment-wide average channel width (updated each minute),

(2) the length of the channel affected, and

(3) the mechanism of change (continuous vs. discrete).

We classified channel displacement using three thresholds. Shifts less than or equal to 0.25 of the average channel width were considered negligible, displacements between 0.25 and 1.0 indicated moderate change, and those exceeding 1.0 times the channel width indicated a high degree of channel relocation. The mechanism of change was determined by the degree of overlap in flow cells between consecutive images. Fewer than 80% overlap implies a discrete (avulsive) jump, whereas higher overlap indicates continuous lateral migration (Fig. 7).

Based on the section-wise classification, fan-scale behavior was determined by combining changes across the up-fan, mid-fan, and down-fan sections. Table 1 summarizes three avulsion modes— complete, partial, and localized— based on whether

https://doi.org/10.5194/egusphere-2025-5934
Preprint. Discussion started: 11 February 2026

Table 2. Summary of average displacement and frequency by channel behavior

Channel Behavior	Frequency	Mean Displacement	Std Deviation
1	4	3.09	2.9
2	15	1.04	0.3
3	14	0.55	0.15
4	7	0.74	0.29
5	23	0.43	0.2
6	95	0.21	0.08
7	170	0.08	0.04

high-magnitude, discrete displacements (>1.0 channel widths) affect one, two, or all three fan sections. A similar threefold classification applies to lateral migrations when displacements exceed 0.25 channel widths but maintain continuity above 80% from one time step to the next.

3.4 Channel Displacement Statistics and Physical Interpretation

Table 2 summarizes the frequency and displacement statistics for each classified channel behavior, listed in order of increasing mean displacement. Complete avulsions (four events) show the largest average shift (~3 channel widths) and highest variability (±2.90), while partial avulsions (15 events) are more frequent, with moderate mean shifts (~1.04). In contrast, localized avulsions and complete lateral migrations both remain below 1.0 channel width (0.55 and 0.74, respectively), consistent with cases where either (1) a single sector experiences a short but intense jump, or (2) the fan undergoes more continuous reworking without fully abandoning its corridor. Partial and localized lateral migrations exhibit even smaller displacements (0.43 and 0.21), whereas quasi-stable conditions account for just over half (53%) of all observations, with a mean displacement of 0.08.

To examine the buildup of smaller, cumulative shifts between avulsions, we tracked cumulative normalized displacement in each fan sector. After every complete or partial avulsion (i.e., a major reorganization affecting at least two fan sectors), this cumulative sum was reset to zero to delineate the onset of a new “fan reorganization” phase. Localized avulsions were excluded from the reset criterion because they affect only one sector and thus do not fully re-route the main channel. Between 260 min and 350 min, the main channel’s cumulative displacement in the mid-fan/down-fan sectors reached up to ~4.93 channel widths—comparable to a major avulsion in total net shift. Although no single one-minute lateral migration event exceeded the displacement typically associated with an avulsion, over longer timescales, cumulative lateral migration can produce spatial changes on par with those triggered by avulsions.

A comparison of net area changes over two 30-minute intervals—a lateral-migration phase (260–300 min) and an avulsion-dominated phase (450–480 min)—reveals that the absolute area of geomorphic change is 0.33 m^2 vs. 0.41 m^2, respectively (Fig.9). When these values are normalized by the total fan area (1.18 m^2 vs. 1.57 m^2), the corresponding proportions are approximately 28% vs. 26%. Despite the frequent assumption that avulsions produce a more extensive geomorphic footprint, these data indicate that lateral migration can rework a comparably large fraction of the fan surface within the same time frame.

https://doi.org/10.5194/egusphere-2025-5934
Preprint. Discussion started: 11 February 2026

Behavior	Length affected	Displacement (times channel width)	Change type	Example
Complete Avulsion	≥ 2/3	> 1.0	Discrete	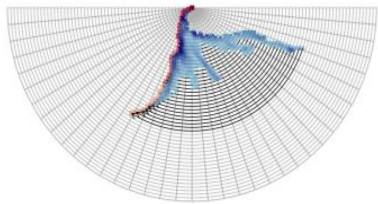
Partial Avulsion	< 2/3 ≥ 1/3	> 1.0	Discrete	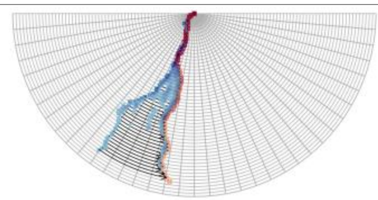
Localized Avulsion	< 1/3	> 1.0	Discrete	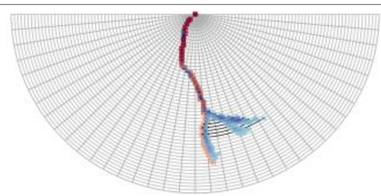
Complete Lateral Migration	≥ 2/3	≥ 0.25	Continuous	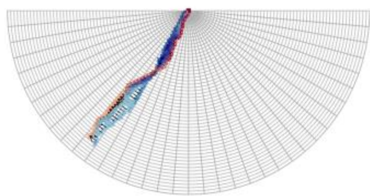
Partial Lateral Migration	< 2/3 ≥ 1/3	≥ 0.25	Continuous	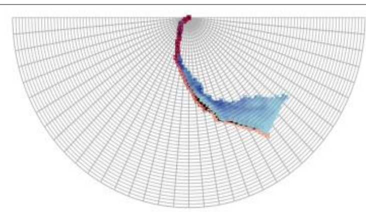
Localized Lateral	< 1/3	≥ 0.25	Continuous	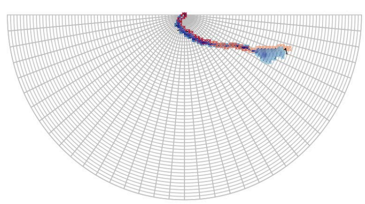

Figure 7. Classification of avulsion and lateral migration modes on experimental alluvial fan.

https://doi.org/10.5194/egusphere-2025-5934
Preprint. Discussion started: 11 February 2026

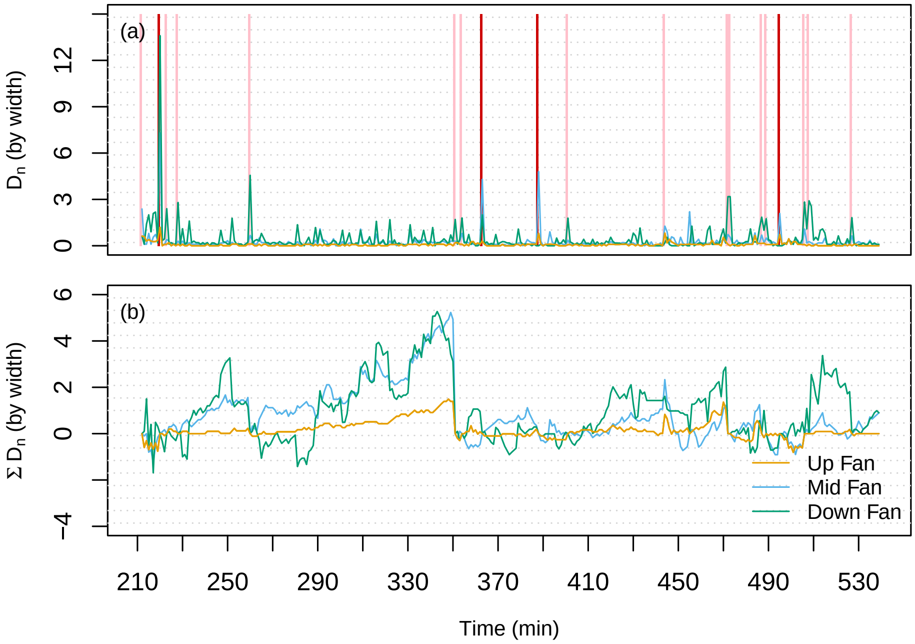

Figure 8. Normalized displacement (Dn) and cumulative Shifts: (a) time series of the per-minute normalized displacement (in each fan sector. Vertical red and pink lines mark complete and partial avulsions, respectively. (b) Cumulative normalized displacement in each sector, reset to zero after complete or partial avulsions that affect at least two sectors.

3.5 Avulsion Timing and State Dependence

Major avulsions (complete or partial; $n = 19$) were identified from the event classification, and their occurrence times were used to compute inter-event intervals Δt. Intervals were highly variable (range = 1–91 minutes; median = 10 minutes; mean = 17.5 minutes), indicating that major avulsions do not exhibit a single characteristic recurrence time over the analyzed interval.

Rather than treating the event series as stationary, we evaluated avulsion timing in relation to the mobility state of the main channel. Using the mobility threshold defined in Section 2.2, the record contains $T_{\mathrm{high}} = 63$ high-mobility minutes and $T_{\mathrm{low}} = 265$ low-mobility minutes (i.e., high mobility occupies $\sim 19\%$ of the time series). All major avulsions occurred during high-mobility minutes ($N_{\mathrm{high}} = 19$, showing that major reorganizations are concentrated into brief high-mobility windows. Importantly, high mobility is not synonymous with major avulsion: only $\sim 30\%$ of high-mobility minutes correspond to major avulsion events $(19/63)$. This framing clarifies the appearance of short clusters in the event sequence: closely spaced avulsions occur when high-mobility conditions persist across multiple consecutive minutes, whereas extended low-mobility intervals separate these windows. Because the mobility state is defined from the displacement metric $\Delta\theta$, this conditioning is not intended as an independent mechanistic test; instead, it provides a compact way to show that major avulsions are confined to a small fraction of the run and occur within short episodes of elevated channel motion.

https://doi.org/10.5194/egusphere-2025-5934
Preprint. Discussion started: 11 February 2026

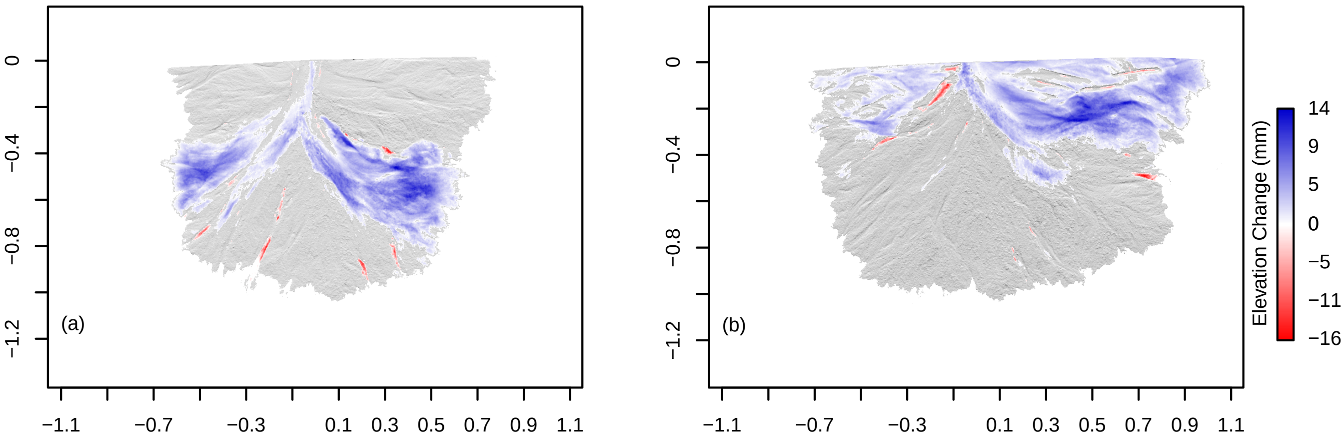

Figure 9. Geomorphic changes for (a) lateral migration from min 270 to 300 min, and (b) avulsion-dominated phases from 450 and 480 min, both overlaid on a hillshade DEM acquired at the subsequent 30-minute scan.

4 Discussion

4.1 Overview of Experimental Fan Evolution and Key Observations

Our principal aims in this study were to: (1) characterize the evolution of a widely graded, non-cohesive alluvial fan under constant boundary conditions, with a focus on the interplay of supply-limited and transport-limited regimes, (2) distinguish discrete (avulsive) relocations from continuous (migratory) shifts using a classification framework that combines displacement magnitude, flow-path continuity, and the spatial extent of reorganization, and (3) assess the timescales of fan-scale reorganizations, exploring whether large-scale avulsions follow predictable cycles or arise spontaneously from autogenic processes. In the following sections, we integrate these findings with existing models of fan-building processes, discussing the role of self-regulating autogenic feedback in driving alluvial-fan evolution.

Our non-cohesive, widely graded experimental alluvial fan reproduced several behaviors reported in earlier fan studies (Schumm et al., 1987; Zarn & Davies, 1994; Bryant et al., 1995; Whipple et al., 1998; Cazanacli et al., 2002), including radial sediment dispersal, episodic channel reorganization, and internally generated (autogenic) variability. At the same time, the broader grain-size range and minute-scale tracking used here resolve short-lived shifts that are difficult to capture in more coarsely sampled experiments.

In our experiment, major avulsions did not exhibit a single recurrence timescale: inter-event intervals were highly variable (1–91 min; median 10 min; mean 17.5 min). When event timing is viewed alongside channel mobility, major avulsions are concentrated within brief high-mobility episodes. High mobility accounts for ~19% of the record (63 of 328 minutes) and contains all 19 major avulsions, while extended low-mobility intervals separate these episodes. Importantly, high mobility is not equivalent to major avulsion—only ~30% of high-mobility minutes coincide with major avulsion events—so elevated mobility appears to be a prerequisite for major reorganization but does not by itself determine whether a major avulsion occurs.

https://doi.org/10.5194/egusphere-2025-5934
Preprint. Discussion started: 11 February 2026

The absence of a characteristic recurrence time and the concentration of events into short mobility episodes argue against a simple, regular cycle controlled solely by fan geometry. This interpretation is consistent with results from Leenman & Eaton (2021) and with broader evidence that constant boundary conditions can still produce nonlinear fan evolution (Muto & Steel, 2001

4.2 A Unified Framework for Classifying Channel Behavior

Despite extensive experimentation on alluvial fans, systematic, quantitative frameworks for distinguishing different types of channel shifts have been scarce. Past works, such as Schumm et al. (1987), described large reorganizations but offered limited metrics for smaller, localized events. Later studies (Jerolmack, 2009; Reitz & Jerolmack, 2012) recognized the importance of both abrupt (avulsive) and gradual (migratory) processes but lacked a standardized approach for comparing results across experiments. In this study, we provided a quantitative classification framework that distinguishes between avulsive (discrete) and lateral (continuous) channel changes using two main parameters: displacement magnitude, measured in multiples of channel width and continuity, defined as the degree of overlap with the previous channel path. Based on quantitative thresholds for channel displacement and flow continuity, translating subjective observations into reproducible categories making it easier to achieve consistent experimental analyses and investigate the underlying physical processes.

A common view in fluvial systems is that sediment aggradation within, or around, the active channel “perches” the flow above the surrounding floodplain, preconditioning it for avulsion (Mohrig et al., 2000). However, deposition alone does not guarantee a full channel abandonment. Applying our classification scheme to experimental observations demonstrates that in a highly dynamic system, such as one we modelled here, large cumulative shifts can arise from repeated continuous migrations rather than singular abrupt events, especially when corridor reworking actively redistributes sediment. Between 260 and 350 minutes, for example, the main channel in our experiment underwent multiple corridor-scale sweeps in the mid-fan/down-fan region, cumulatively reaching ∼4.93 channel widths—on par with a major avulsion in total displacement. Yet these repeated lateral shifts did not involve a sudden reoccupation of a completely different route. Instead, partial migrations and localized reworking continuously scoured and redeposited sediment, preventing the buildup of a high, perched channel.

In our experiment, the nature of channel change was closely tied to the hydraulic regime in the main channel, which alternated between supply-limited and transport-limited conditions. During prolonged supply-limited phases, at least two-thirds of the channel length had sufficient stream power to transport incoming sediment to the fan toe. Any sediment that did accumulate farther down-fan produced only localized impacts, resulting in minimal net aggradation. Consequently, the flow remained within a discrete corridor, yet this corridor itself shifted laterally over time through incremental migration. Although major avulsions occurred only infrequently, repeated corridor reworking through successive minor lateral migrations could ultimately produce a net displacement on par with a single large avulsion. In essence, the channel continuously scoured and redeposited local patches of sediment without building up the broad, persistent deposits that would “perch” it to the point of abrupt abandonment. By contrast, transport-limited conditions—where coarser grains accumulated faster than they could be reworked or bypassed—occasionally generated partial super-elevation or localized slope advantages. These settings favored abrupt, discrete jumps of the main channel. Although some full-scale avulsions were observed, they were mostly confined to

https://doi.org/10.5194/egusphere-2025-5934
Preprint. Discussion started: 11 February 2026

one or two fan sectors rather than extending from the apex to the toe. This behavior aligns with findings by (Cazanacli et al., 2022) and (Clarke et al., 2010), who similarly documented smaller-scale reorganizations that left large parts of the fan surface unaffected.

According to (Mohrig et al., 2000) and (Jerolmack and Mohrig, 2007), the time between avulsions in single-thread rivers can be approximated by the formula $T_{\text{avulsion}} = H/V_a$, where H is the channel depth and V_a is the vertical aggradation rate. While this formula offers a useful first-order guide, our experiments show that not all sediment deposition triggers avulsion. Frequent lateral reworking and local bar formation can repeatedly reset channel geometry before the channel becomes fully perched. Consequently, the H/V_a relationship underestimates the importance of small-scale, autogenic adjustments—particularly in highly mobile, widely graded systems where corridor confinement delays or even prevents large-scale avulsions.

4.3 Sediment Connectivity and Partial Coupling

Beyond distinguishing lateral migrations from avulsions, our data illustrate how sediment connectivity exerts a first-order control on fan dynamics (Harvey, 2010). In natural fan systems, three end-member connectivity states are often cited: buffered systems, where incoming sediment is mainly stored on the fan, leading to high aggradation and minimal sediment export; partially coupled systems, in which some sediment bypasses the fan while the remainder is deposited mid-fan or proximally; and fully coupled systems, where sediment passes freely through the fan, resulting in minimal net storage. Although these concepts are usually discussed in the context of external forcing (tectonics, climate), our experiments show that purely autogenic processes—operating under constant water and sediment supply—can cause the fan to oscillate between more "buffered" and more "partially coupled" states. During supply-limited intervals, the channel effectively transported a notable fraction of the incoming sediment off the fan, indicating partial coupling; local deposits formed but did not cause significant net aggradation. Conversely, during transient transport-limited phases, coarser grains began to accumulate, producing short-lived "buffering" in specific fan sectors. Occasionally, this buffering was sufficient to trigger abrupt channel jumps. Our results suggest that these oscillations between connectivity states coincide with abrupt drops in channel mobility, which, in turn, determine the preferred locations of avulsion nodes and ultimately drive shifts in alluvial style.

4.4 Role of Widely Graded Sediment in Channel Stability

Although our grain-size distribution was nominally non-cohesive, it differed substantially from the narrowly graded sand mixtures used in previous experiments (Reitz and Jerolmack, 2012; Hamilton et al., 2013; Reitz et al., 2010; Carlson et al., 2018). The presence of coarse particles introduced a degree of bed stability, reducing the occurrence of the sheet flow often observed with single-sized sediment (Whipple et al., 1998). Larger clasts nucleated bars and funnelled the flow into channelized corridors rather than allowing it to spread uniformly across the fan surface. These observations align with findings by (Booker and Eaton, 2020), (MacKenzie and Eaton, 2017), and (MacKenzie et al., 2018), who show that large grains can reduce bed mobility, effectively locking portions of the channel and altering the frequency or style of channel adjustments. In our experiments, this stabilization effect worked in tandem with lower sediment feed rates to facilitate corridor sweeps that continuously eroded and reworked nascent bars, preventing large-scale backfilling. By contrast, (Leenman and Eaton, 2021) demonstrated that higher

https://doi.org/10.5194/egusphere-2025-5934
Preprint. Discussion started: 11 February 2026

sediment discharge can promote more frequent avulsions; faster aggradation raises the active channel relative to the fan surface, lowering the threshold for abrupt shifts. Thus, even modest differences in sediment supply can tip the balance between stable corridor migration and repeated channel avulsion in systems with wide grain-size distributions (Bryant et al., 1995; Ashworth et al., 2004).

5 Conclusions

Our experiments on a widely graded, non-cohesive alluvial fan under constant boundary conditions highlight the complex interplay between supply-limited and transport-limited regimes in shaping channel reorganization. Using a quantitative classification framework—based on displacement magnitude (relative to channel width) and flow continuity—we differentiate abrupt avulsive from continuous lateral channel shifts, revealing that large net displacements need not arise from singular, fan-wide avulsions. Instead, repeated corridor sweeps can accumulate to match the net effect of a single major jump, indicating how frequent, moderate-scale migrations can dominate fan evolution even when avulsion conditions are theoretically present.

Although sediment aggradation is widely recognized as a key factor in channel perching, our data confirm that deposition alone does not guarantee complete channel abandonment. Partial blockage, localized bar formation, and corridor confinement repeatedly reset the channel geometry, delaying or entirely disturbing the cyclic backfilling.

From the perspective of sediment connectivity, our fan oscillated between partially coupled and locally buffered states strictly through internal processes, aligning with previous observations that fans need not rely on external forcing to achieve major reconfigurations. In terms of hazard implications, both corridor sweeps and partial avulsions can affect comparably large areas of the fan. However, the unpredictability of avulsion locations poses a distinct challenge, whereas lateral migration—though still dynamic—tends to remain adjacent to the existing channel, offering somewhat clearer pathways for hazard assessment and mitigation.

Ultimately, our results refine the understanding of alluvial-fan evolution by showing that high lateral mobility and wide grain-size distributions promote incremental corridor reworking, punctuated by occasional abrupt channel jumps. This does not diminish the importance of avulsions for shaping the long-term development and stratigraphic record of major fluvial systems. Instead, it emphasizes that repeated, smaller-scale migrations can significantly redistribute sediment and prolong the interval before an avulsion occurs—especially when total aggradation remains below the threshold set by channel depth. In highly dynamic systems with abundant bedload, these processes can sustain corridor migration and temporarily avoid avulsion. Recognizing the contribution of frequent, moderate-scale reworking and larger, discrete channel shifts is crucial for hazard assessments on modern alluvial fans and for interpreting the sedimentary signatures of ancient fan deposits.

https://doi.org/10.5194/egusphere-2025-5934
Preprint. Discussion started: 11 February 2026

Code and data availability. The full source data for this study exceed 1 TB in size and are therefore not hosted online. Code and sample data are openly available at: https://github.com/Nastarannmt. The complete datasets are available from the corresponding author upon reasonable request.

Video supplement. The supplementary video presents a time-lapse sequence from 210 to 540 minutes of the 9-hour experiment. The initial 3.5 hours, during which the fan developed its baseline morphology, are excluded. The video therefore focuses on the period analyzed in the study, capturing the active phases of channel migration, reorganization, and avulsion.

Author contributions. NN designed and carried out the experiments, processed optical-flow maps and DEMs, analyzed results, and drafted the manuscript. BRE supervised the study, contributed to interpretation, and edited the manuscript. SD provided technical guidance and contributed to analysis and manuscript revisions.

Competing interests. The authors declare no competing interests.

Disclaimer. The authors used AI-assisted proofreading tools to improve grammar and clarity. All interpretations and conclusions are solely those of the authors.

Acknowledgements. Experimental construction and equipment purchase were supported by an NSERC Discovery Grant awarded to B. Eaton. N. Nematollahi was supported by a Four Year Doctoral Fellowship from the University of British Columbia. We thank Anya Leenman for her in-depth reviews, which greatly improved the clarity and quality of the manuscript.

https://doi.org/10.5194/egusphere-2025-5934
Preprint. Discussion started: 11 February 2026

References

Ashmore, P.: 9.17 Morphology and Dynamics of Braided Rivers, in: Treatise on Geomorphology, pp. 289–312, Elsevier, ISBN 978-0-08-088522-3, https://doi.org/10.1016/B978-0-12-374739-6.00242-6, 2013.

Ashmore, P. E.: How do gravel-bed rivers braid?, Canadian Journal of Earth Sciences, 28, 326–341, https://doi.org/10.1139/e91-030, 1991.

Booker, W. H. and Eaton, B. C.: Stabilising large grains in self-forming steep channels, Earth Surface Dynamics, 8, 51–67, https://doi.org/10.5194/esurf-8-51-2020, publisher: Copernicus GmbH, 2020.

Bradski, G.: The OpenCV Library, in: Dr. Dobb's Journal of Software Tools, 2000.

Bryant, M., Falk, P., and Paola, C.: Experimental study of avulsion frequency and rate of deposition, Geology, 23, 365–368, https://doi.org/10.1130/0091-7613(1995)023<0365:ESOAFA>2.3.CO;2, 1995.

Bufe, A., Turowski, J. M., Burbank, D. W., Paola, C., Wickert, A. D., and Tofelde, S.: Controls on the lateral channel-migration rate of braided channel systems in coarse non-cohesive sediment, Earth Surface Processes and Landforms, 44, 2823–2836, https://doi.org/10.1002/esp.4710, _eprint: https://onlinelibrary.wiley.com/doi/pdf/10.1002/esp.4710, 2019.

Bull, W. B.: Threshold of critical power in streams, GSA Bulletin, 90, 453–464, https://doi.org/10.1130/0016-7606(1979)90<453:TOCPIS>2.0.CO;2, 1979.

Burge, L. M.: Stability, morphology and surface grain size patterns of channel bifurcation in gravel–cobble bedded anabranching rivers, Earth Surface Processes and Landforms, 31, 1211–1226, https://doi.org/10.1002/esp.1325, _eprint: https://onlinelibrary.wiley.com/doi/pdf/10.1002/esp.1325, 2006.

Carlson, B., Piliouras, A., Muto, T., and Kim, W.: Control of Basin Water Depth On Channel Morphology and Autogenic Timescales in Deltaic Systems, Journal of Sedimentary Research, 88, 1026–1039, https://doi.org/10.2110/jsr.2018.52, 2018.

Cazanacli, D., Paola, C., and Singh, A.: Sediment Load and Grain Size Controls on Channel Migration Patterns in Experimental Deltas, Journal of Geophysical Research: Earth Surface, 127, e2021JF006 402, https://doi.org/10.1029/2021JF006402, 2022.

Church, M. and Jakob, M.: What Is a Debris Flood?, Water Resources Research, 56, e2020WR027 144, https://doi.org/10.1029/2020WR027144, _eprint: https://onlinelibrary.wiley.com/doi/pdf/10.1029/2020WR027144, 2020.

Clarke, L., Quine, T. A., and Nicholas, A.: An experimental investigation of autogenic behaviour during alluvial fan evolution, Geomorphology, 115, 278–285, https://doi.org/10.1016/j.geomorph.2009.06.033, 2010.

Constantine, J. A., Dunne, T., Ahmed, J., Legleiter, C., and Lazarus, E. D.: Sediment supply as a driver of river meandering and floodplain evolution in the Amazon Basin, Nature Geoscience, 7, 899–903, https://doi.org/10.1038/ngeo2282, 2014.

Davidson, S. L. and Eaton, B. C.: Beyond Regime: A Stochastic Model of Floods, Bank Erosion, and Channel Migration, Water Resources Research, 54, 6282–6298, https://doi.org/10.1029/2017WR022059, 2018.

Farneback, G.: Fast and accurate motion estimation using orientation tensors and parametric motion models, in: Proceedings 15th International Conference on Pattern Recognition. ICPR-2000, vol. 1, pp. 135–139 vol.1, https://doi.org/10.1109/ICPR.2000.905291, iSSN: 1051-4651, 2000.

Fonstad, M. A., Dietrich, J. T., Courville, B. C., Jensen, J. L., and Carbonneau, P. E.: Topographic structure from motion: a new development in photogrammetric measurement, Earth Surface Processes and Landforms, 38, 421–430, https://doi.org/10.1002/esp.3366, _eprint: https://onlinelibrary.wiley.com/doi/pdf/10.1002/esp.3366, 2013.

https://doi.org/10.5194/egusphere-2025-5934
Preprint. Discussion started: 11 February 2026

Hamilton, P. B., Strom, K., and Hoyal, D. C. J. D.: Autogenic incision-backfilling cycles and lobe formation during the growth of alluvial fans with supercritical distributaries, Sedimentology, 60, 1498–1525, https://doi.org/10.1111/sed.12046, _eprint: https://onlinelibrary.wiley.com/doi/pdf/10.1111/sed.12046, 2013.

Harvey, A. M.: Local Buffers to the Sediment Cascade: Debris Cones and Alluvial Fans, in: Sediment Cascades, pp. 153–180, John Wiley & Sons, Ltd, ISBN 978-0-470-68287-6, https://doi.org/10.1002/9780470682876.ch6, section: 6 _eprint: https://onlinelibrary.wiley.com/doi/pdf/10.1002/9780470682876.ch6, 2010.

Hooke, R.: Model Geology: Prototype and Laboratory Streams: Discussion, GSA Bulletin, 79, 391–394, https://doi.org/10.1130/0016-7606(1968)79[391:MGPALS]2.0.CO;2, 1968.

Jerolmack, D. J.: Conceptual framework for assessing the response of delta channel networks to Holocene sea level rise, Quaternary Science Reviews, 28, 1786–1800, https://doi.org/10.1016/j.quascirev.2009.02.015, 2009.

Jerolmack, D. J. and Mohrig, D.: Conditions for branching in depositional rivers, Geology, 35, 463, https://doi.org/10.1130/G23308A.1, 2007.

Jobe, Z. R., Howes, N. C., and Auchter, N. C.: Comparing submarine and fluvial channel kinematics: Implications for stratigraphic architecture, Geology, 44, 931–934, https://doi.org/10.1130/G38158.1, 2016.

Leenman, A. and Eaton, B.: Mechanisms for avulsion on alluvial fans: Insights from high-frequency topographic data, Earth Surface Processes and Landforms, 46, 1111–1127, https://doi.org/10.1002/esp.5059, 2021.

MacKenzie, L. G. and Eaton, B. C.: Large grains matter: contrasting bed stability and morphodynamics during two nearly identical experiments, Earth Surface Processes and Landforms, 42, 1287–1295, https://doi.org/10.1002/esp.4122, _eprint: https://onlinelibrary.wiley.com/doi/pdf/10.1002/esp.4122, 2017.

MacKenzie, L. G., Eaton, B. C., and Church, M.: Breaking from the average: Why large grains matter in gravel-bed streams, Earth Surface Processes and Landforms, 43, 3190–3196, https://doi.org/10.1002/esp.4465, _eprint: https://onlinelibrary.wiley.com/doi/pdf/10.1002/esp.4465, 2018.

Mackey, S. D. and Bridge, J. S.: Three-dimensional model of alluvial stratigraphy; theory and applications, Journal of Sedimentary Research, 65, 7–31, https://doi.org/10.1306/D42681D5-2B26-11D7-8648000102C1865D, 1995.

Martin, J., Sheets, B., Paola, C., and Hoyal, D.: Influence of steady base-level rise on channel mobility, shoreline migration, and scaling properties of a cohesive experimental delta, Journal of Geophysical Research: Earth Surface, 114, 2008JF001 142, https://doi.org/10.1029/2008JF001142, 2009.

Miller, K. L., Kim, W., and McElroy, B.: Laboratory Investigation on Effects of Flood Intermittency on Fan Delta Dynamics, Journal of Geophysical Research: Earth Surface, 124, 383–399, https://doi.org/10.1029/2017JF004576, _eprint: https://onlinelibrary.wiley.com/doi/pdf/10.1029/2017JF004576, 2019.

Mohrig, D., Heller, P. L., Paola, C., and Lyons, W. J.: Interpreting avulsion process from ancient alluvial sequences: Guadalope-Matarranya system (northern Spain) and Wasatch Formation (western Colorado), GSA Bulletin, 112, 1787–1803, https://doi.org/10.1130/0016-7606(2000)112<1787:IAPFAA>2.0.CO;2, 2000.

R Core Team: R: A Language and Environment for Statistical Computing, R Foundation for Statistical Computing, Vienna, Austria, https://www.R-project.org/, 2025.

Reitz, M. D. and Jerolmack, D. J.: Experimental alluvial fan evolution: Channel dynamics, slope controls, and shoreline growth, Journal of Geophysical Research: Earth Surface, 117, 2011JF002 261, https://doi.org/10.1029/2011JF002261, 2012.

https://doi.org/10.5194/egusphere-2025-5934
Preprint. Discussion started: 11 February 2026

Reitz, M. D., Jerolmack, D. J., and Swenson, J. B.: Flooding and flow path selection on alluvial fans and deltas, Geophysical Research Letters, 37, 2009GL041 985, https://doi.org/10.1029/2009GL041985, 2010.

Schumm, S. A., Mosley, M. P., and Weaver, W.: Experimental fluvial geomorphology, https://www.osti.gov/biblio/6211294, publisher: John Wiley and Sons Inc.,New York, NY, 1987.

Slingerland, R. and Smith, N. D.: RIVER AVULSIONS AND THEIR DEPOSITS, Annual Review of Earth and Planetary Sciences, 32, 257–285, https://doi.org/10.1146/annurev.earth.32.101802.120201, 2004.

Sylvester, Z., Durkin, P., and Covault, J. A.: High curvatures drive river meandering, Geology, 47, 263–266, https://doi.org/10.1130/G45608.1, 2019.

Westoby, M. J., Brasington, J., Glasser, N. F., Hambrey, M. J., and Reynolds, J. M.: 'Structure-from-Motion' photogrammetry: A low-cost, effective tool for geoscience applications, Geomorphology, 179, 300–314, https://doi.org/10.1016/j.geomorph.2012.08.021, 2012.

Whipple, K. X., Parker, G., Paola, C., and Mohrig, D.: Channel Dynamics, Sediment Transport, and the Slope of Alluvial Fans: Experimental Study, The Journal of Geology, 106, 677–694, https://doi.org/10.1086/516053, publisher: The University of Chicago Press, 1998.

Wickert, A. D., Martin, J. M., Tal, M., Kim, W., Sheets, B., and Paola, C.: River channel lateral mobility: metrics, time scales, and controls, Journal of Geophysical Research: Earth Surface, 118, 396–412, https://doi.org/10.1029/2012JF002386, 2013.

Wolman, MG; Miller, J.: Magnitude and frequency of forces in geomorphic processes, Journal of Geology, 68, 54–74, 1960.